ATMOSPHERIC AND OCEANIC SCIENCE LETTERS, 2014, VOL. 7, NO. 1, 1–6

Sensitivity of Precipitation in Aqua-Planet Experiments with an AGCM

YU Hai-Yang[1,2], BAO Qing[1], ZHOU Lin-Jiong[1,2], WANG Xiao-Cong[1], and LIU Yi-Min[1]

[1] *State Key Laboratory of Numerical Modeling for Atmospheric Sciences and Geophysical Fluid Dynamics (LASG), Institute of Atmospheric Physics, Chinese Academy of Sciences, Beijing 100029, China*

[2] *Graduate University of Chinese Academy of Sciences, Beijing 100049, China*

Received 26 March 2013; revised 19 April 2013; accepted 2 May 2013; published 16 January 2014

Abstract The sensitivity of precipitation was studied by conducting control aqua-planet experiments (APEs) with a model to determine atmospheric general circulation. The model includes two versions: that with a spectral dynamical core (SAMIL) and that with a finite-volume dynamical core (FAMIL). Three factors were investigated including dynamical core, time-step length, and horizontal resolution. Numerical results show that the dynamical core significantly affects the structure of zonal averaged precipitation. FAMIL exhibited an equatorial precipitation belt with a single narrow peak, and SAMIL showed a broader belt with double peaks. Moreover, the time step of the model physics is shown to affect the zonal-averaged tropical convective precipitation ratio such that a longer time step leads to more production and consumption of convective available potential energy and convection initiated away from the equator, which corresponds to equatorial double peaks of precipitation. Further, precipitation is determined to be sensitive to horizontal resolution such that higher horizontal resolution allows for more small-scale kinetic energy to be resolved and leads to a broader probability distribution of low-level vertical velocity. This process results in heavier rainfall and convective precipitation extremes in the tropics.

Keywords: aqua-planet experiment, precipitation sensitivity, dynamical core, horizontal resolution, time step

Citation: Yu, H.-Y., Q. Bao, L.-J. Zhou, et al., 2014: Sensitivity of precipitation in aqua-planet experiments with an AGCM, *Atmos. Oceanic Sci. Lett.*, **7**, 1–6, doi:10.3878/j.issn.1674-2834.13.0033.

1 Introduction

The hydrological cycle involves the exchange of energy and has a significant impact on life and ecosystems on Earth. Precipitation is one of the most important physical parameters of this cycle and is a crucial index used for comprehensive modeling. Thus, a sensitivity study of precipitation can effectively explain the physical processes of the model and significantly improve its performance.

Previous research has shown that the major factors affecting precipitation include orography (Houze, 2012), horizontal and vertical resolution (Pope and Stratton, 2002), time step (Williamson and Olson, 2003), and the parameterization scheme (Hess et al., 1993). Some studies demonstrated that patterns of precipitation could be a response to the large-scale atmospheric circulation (Arakawa and Schubert, 1974), which is mainly determined by the dynamical core. However, few studies have focused on the impacts of the dynamic core on precipitation (Williamson and Olson, 2003).

The aqua-planet experiment (APE) (Neale and Hoskins, 2000) is a suitable coordinated numerical experiment to investigate the effects of dynamical core on the sensitivity of precipitation. On the basis of APEs, many previous studies explored the sensitivity of precipitation by using an atmospheric general circulation model (AGCM): Williamson and Olson (2003) studied the dependence of precipitation on time step; Williamson (2008) documented convergence problems of precipitation with increasing horizontal resolution; Li et al. (2011) studied the impact of horizontal resolution on the precipitation extremes in aqua-planet simulations.

In this study, an AGCM with two dynamical cores was used in an APE to determine their effects on precipitation. We considered three important factors including the numerical method used to model the core, the length of time step, and horizontal resolution. The AGCM is described in section 2, and section 3 shows the specific experimental design. A detailed analysis of the numerical results is provided in section 4. Finally, we offer the conclusions and discussions in section 5.

2 Model description

The AGCM used in this study was the Finite-volume/Spectral Atmospheric Model (F/SAMIL), which was developed in by State Key Laboratory of Numerical Modeling for Atmospheric Sciences and Geophysical Fluid Dynamics (LASG) of the Institute of Atmospheric Physics (IAP). F/SAMIL consists of two versions including that with a spectral dynamical core (SAMIL) and that with a finite-volume dynamical core (FAMIL). Both share a common physical package.

The early version of SAMIL was a nine-level rhomboidal truncated spectral model that and was capable of simulating climate mean states as well as monsoon onset and interannual variability (Wu et al., 1996; Wang et al., 2004). In addition to its usage for aqua-planet research (Wang et al., 2008), SAMIL improvements include 26 levels vertically and rhombic truncation with the maximum wavenumber 42 (R42) horizontally with parallel computation (Wang and Wang, 2006). Moreover, it is combined with other model components to form a climate system model widely used for climate change and dy-

Corresponding author: BAO Qing, baoqing@mail.iap.ac.cn

namic studies (Bao et al., 2013; Wei and Bao, 2012).

FAMIL is the latest version of F/SAMIL and contains a finite volume dynamical core (Lin, 2004). The key characters of FAMIL include flux-form semi-Lagrangian (FFSL) transport scheme (Wang et al., 2013), vertical Lagrangian control-volume discretion, and achievement of dynamical core on the cubed-sphere grid, which overcomes the polar problem and applies parallel computation efficiently (Putman and Lin, 2007). Numerical testing by a supercomputer verified its efficient computing performance (Zhou et al., 2012).

The vertical grids in F/SAMIL are 26-level hybrid coordinates from the Earth's surface to approximately 3 hPa. Table 1 shows the available resolutions. The physical package, is shared with SAMIL, has full parameterization modules including the main processes in the atmosphere (Table 1). In particular, the cumulus parameterization in F/SAMIL is a modified mass flux scheme, which was first designed by Tiedtke (1989), and uses convective available potential energy (CAPE) as the closure hypothesis (Nordeng, 1994).

3 Experiment design

APEs were conducted in this study to avoid complications from the underlying surface. Following the approach designed by Neale and Hoskins (2000), the model included a full parameterization suite and was designed for simple surface conditions that essentially assumed the earth is covered with water. That is, the effects of mountains, land, and sea ice were disregarded. The sea surface temperature (SST) was specified with special geometries such as zonal symmetry. A diurnal cycle of solar radiation was included with the sun remaining over the equator. Because the only radiatively active aerosols detected were greenhouse species symmetric about the equator, the aqua-planet climate is also expected to be symmetric about the equator.

We followed the control case of Neale and Hoskins (2000), in which the SST is defined in °C for latitude only:

$$\mathrm{SST}(\lambda,\phi)=\begin{cases}27\left[1-\sin^2(3\phi/2)\right] & if\ |\phi|<60^\circ \\ 0 & if\ |\phi|\geq 60^\circ\end{cases},$$

where λ and φ are longitude and latitude, respectively.

The simulations began from an idealized state and ran for two years. The first year was treated as the "spin-up" period because the model transitioned from its initial conditions to the aqua-planet climate in less than two months (Williamson, 2008). All parameters in the physical packages remained untuned because no known correct solution was available for comparison (Williamson, 2008). Nevertheless, it was determined that the simple environment of the APE provided the necessary conditions for examining the sensitivity of model simulations such as precipitation.

4 Sensitivity analysis

On the basis of the control APEs with F/SAMIL, the sensitivity of precipitation was analyzed relative to the three aforementioned factors. Generally, more global averaged precipitation was simulated by SAMIL than that

Table 1 Finite-volume/Spectral Atmospheric Model (F/SAMIL) for atmospheric general circulation.

	SAMIL			FAMIL		
Dynamical core	Spectral method			Finite-volume method		
Advection scheme	Spectral transform			FFSL transport scheme		
Time slices	Semi-implicit (three levels)			Explicit (two levels)		
Grid type	Gaussian grid			Cubed-sphere grid		
Horizontal resolution	R42	R85	R106	C48	C96	C192
Latitude × Longitude (°)	2.8×1.67	1.4×0.84	1.1×0.68	~2×2	~1×1	~0.5×0.5
Max grid length (km)	313	156	125	231	116	58
Min grid length (km)	6.9	1.75	1.1	163	82	41
Equivalent grid length* (km)	192	96	77	192	96	48
4-order diffusion coefficient	1.0e16	1.0e15	5.0e14	–	–	–
4-order damping coefficient	–	–	–	0.16	0.16	0.16
Time step (s)	600	300	300	1800	1200	900
Vertical coordinate	Hybrid coordinate (26 levels)					
Radiation	(Sun and Rikus, 1999; Li, 2009)					
Boundary layer	High-order closure scheme (Brinkop and Roeckner, 1995)					
Gravity wave drag	Multiple gravity wave drag scheme (Gregory et al., 1997)					
Convection	Mass flux cumulus parameterization (Song, 2005)					
Microphysics	None					

*Calculated by the grid points on the Earth: $\sqrt{4\pi R^2/n}$. R is the radius of the Earth, and n is the amount of global grid points.

by FAMIL at 0.2–0.4 mm d^{-1}. The global averaged precipitation, particularly that on a large scale, increased with increasing horizontal resolution (Table 2). In this section, we will show that a decrease in time step associated with an increase in horizontal resolution may be the main factor in the change of the partition of precipitation.

For the zonal averaged pattern, SAMIL simulated a broad equatorial precipitation belt with double peaks, while FAMIL simulated a stronger single narrow peak (Fig. 1). An increase in horizontal resolution associated with a decrease in time step resulted in stronger peaks of total precipitation in SAMIL but weak changes in FAMIL. Thus, FAMIL likely gives a more reasonable result such that the equatorial convective precipitation decreases while large-scale precipitation peaks increases with a rise in horizontal resolution. Generally, the dynamical core is the primary influence of the structure of precipitation, while the horizontal resolution, which is associated with time step, is a secondary factor and affects magnitude. Actually, the resolution change consists of many factors that can be isolated from each other (Williamson, 2008). In this study, we considered time step separately and combined the effects of grid interval, truncation in SAMIL only, and diffusive smoothing together as a pure resolution effect.

4.1 Sensitivity of dynamical core

As shown in Fig. 2, SAMIL R42 simulated a broad ascending belt with double peaks in the tropics (10°S–10°N), while FAMIL C48 (global cubed-sphere grid with 48×48 cells on each tile) showed a much stronger and narrower belt. The mean vertical profiles of equatorial vertical velocity (5°S–5°N) in Figs. 2a and 2c also show that SAMIL R42 simulated a lower (~ 850 hPa) and weaker (–0.062 Pa s^{-1}) major peak of upward motion than that of FAMIL C48 (–0.097 Pa s^{-1} at ~ 780 hPa) and a weaker (–0.048 Pa s^{-1}) but higher (~ 340 hPa) secondary peak than that of FAMIL C48 (–0.072 Pa s^{-1} at ~ 400 hPa).

Table 2 Time- and global-averaged precipitation determined by aqua-planet experiments (APEs) with F/SAMIL. Units: mm d^{-1}.

	SAMIL			FAMIL		
	R42	R85	R106	C48	C96	C192
Total	2.30	2.53	2.58	2.14	2.18	2.20
Convective	1.16	1.10	1.08	1.05	0.98	0.90
Large-scale	1.14	1.43	1.50	1.09	1.20	1.29

These results indicate that FAMIL has a much stronger sensitive response on the specified maximum SST at the equator. Further studies showed that the equatorial air temperature on the bottom model level of FAMIL C48 was lower than that of SAMIL R42 by 0.8 K, indicating higher sensible heating over the tropical ocean surface. Meanwhile, the tropical moisture content near the ocean surface in FAMIL C48 was more than that of SAMIL R42 by ~ 2 g kg^{-1}. These two factors led to a larger equatorial CAPE (Figs. 2b and 2d), thus stronger convective precipitation over tropics in FAMIL C48 (Figs. 1b and 1e). Furthermore, the stronger latent heating from condensation accelerated the equatorial ascending and induced additional low-level moisture convergence. This type of positive feedback could explain the narrower equatorial precipitation belt with a single peak in FAMIL C48 rather than the broad weak belt with double peaks in SAMIL R42 (Figs. 1a and 1d). Finally, the equatorial divergence of moisture flux in FAMIL C48 corresponding to the vertical velocity was substantially more concentrated and stronger than that of SAMIL R42 (not shown), which indicates that the advection scheme may have played an additional role in influencing the equatorial precipitation (Wang et al., 2013). Further experiments are needed to demonstrate the effects of the advection scheme.

4.2 Sensitivity of time step

The time step in this analysis represents the coupling frequency between the dynamical core and the physical package only (Table 1) because previous studies indicated that the precipitation in APE does not have significant

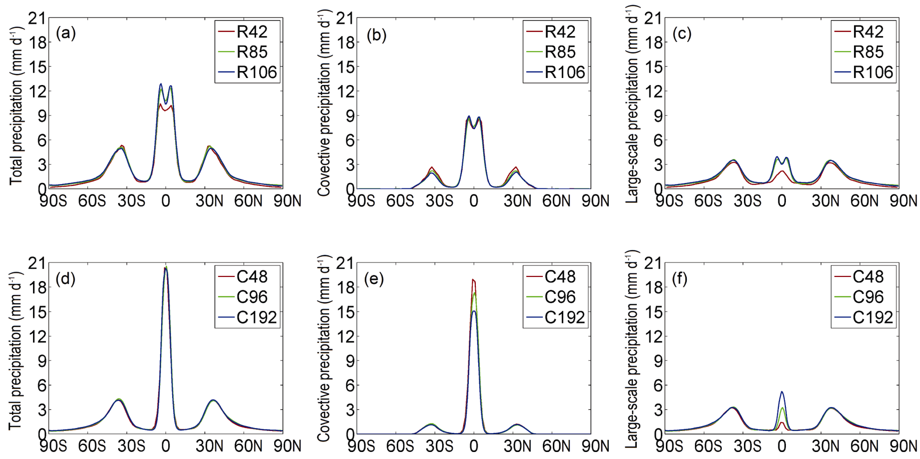

Figure 1 Time- and zonal-averaged total precipitation (left column), convective precipitation (middle column), and large-scale precipitation (right column) determined by aqua-planet experiments (APEs) including atmospheric models with a spectral dynamical core (SAMIL, upper panels) and that with a finite-volume dynamical core (FAMIL, bottom panels).

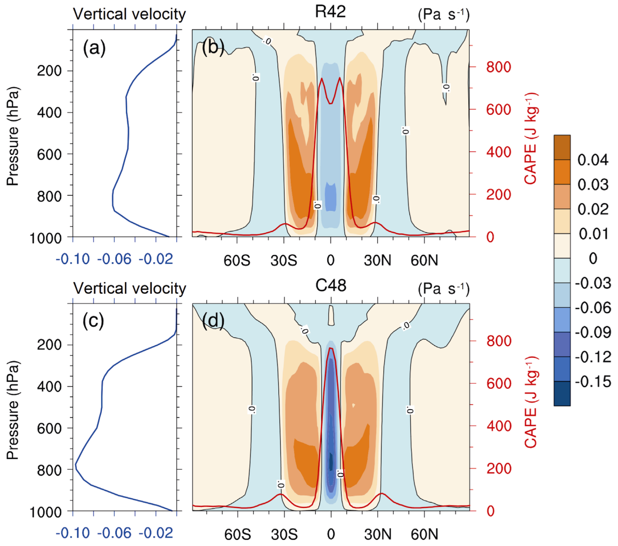

Figure 2 Averaged vertical profiles of equatorial vertical velocity (5°S–5°N) determined by APEs (units: Pa s^{-1}) with (a) an atmospheric model with a SAMIL R42 and (c) that with a FAMIL C48. The height-latitude cross section shows vertical velocity from APEs determined by (b) SAMIL R42 and (d) FAMIL C48. Red lines represent zonal-averaged convective available potential energy (CAPE) (units: J kg^{-1}) from APEs of (b) SAMIL R42 and (d) FAMIL C48.

sensitivity on sub-time step in the dynamical core (Williamson and Olson, 2003).

The equatorial maximum precipitation increased with a decrease in time step for each specific horizontal resolution (Figs. 3a–d), which primarily contributed to the sensitivity of precipitation to the horizontal resolution (Fig. 1). Moreover, the time step had a remarkable influence on the structure of precipitation in FAMIL but nearly no impact on that of SAMIL. Because the two share the same physical package, it is indicated that the dynamical core of FAMIL (e.g., advection scheme) is more sensitive to the coupling frequency with physical processes that that of SAMIL. For FAMIL with high resolution (C96 and C192), the single equatorial peak of precipitation split into double peaks with an increase in time step (Figs. 3c and 3d). The increased precipitation farther from the equator appeared to ascend because additional water was placed into the atmosphere by the surface exchange parameterizations with a longer time step (Williamson and Olson, 2003).

When the time step was increased, more water vapor was evaporated from the equatorial warm ocean rather than being transported to the equator by the advection scheme. The additional moisture had ample time to be distributed by vertical diffusion, which resulted in a larger CAPE and stronger convection over and away from the equator. Furthermore, once the convection farther from the equator was initiated, positive feedback led to enhanced convection, which consumed more low-level moisture convergence and resulted in double peaks of precipitation. This hypothesis is proved by Fig. 3e. As the time step increases, the fraction of tropical convective precipitation also increases, particularly in the region away from the equator.

In addition, the cumulus parameterization in F/SAMIL included a fixed relaxation time scale of the consumption rate of CAPE. During a longer time step, more CAPE was consumed in the convective adjustment; thus, the air became more stable prior to the formation of large-scale condensation. This process led to a smaller fraction of large-scale precipitation and a larger convective fraction (Figs. 3e–h).

4.3 Impacts of the horizontal resolution

Two series of APEs were conducted for F/SAMIL with the same time step but different horizontal resolutions for each group. All of the spectral versions of SAMIL R42, R85, and R106 used the same time step of 300 s; that for FAMIL C48, C96, and C192 was 1800 s (Fig. 4).

Precipitation frequency, rather than zonal averaged pattern, showed remarkable sensitivity to the horizontal resolution. Precipitation extremes, particularly those of convective precipitation such as the 99th percentile of probability distribution of daily precipitation, increased with increasing horizontal resolution (Figs. 4d and 4h). This result is attributed mainly to an increase in dynamical extremes such as those of vertical velocity. Many studies have shown that daily precipitation has a high linear correlation with daily vertical velocity (Li et al.,

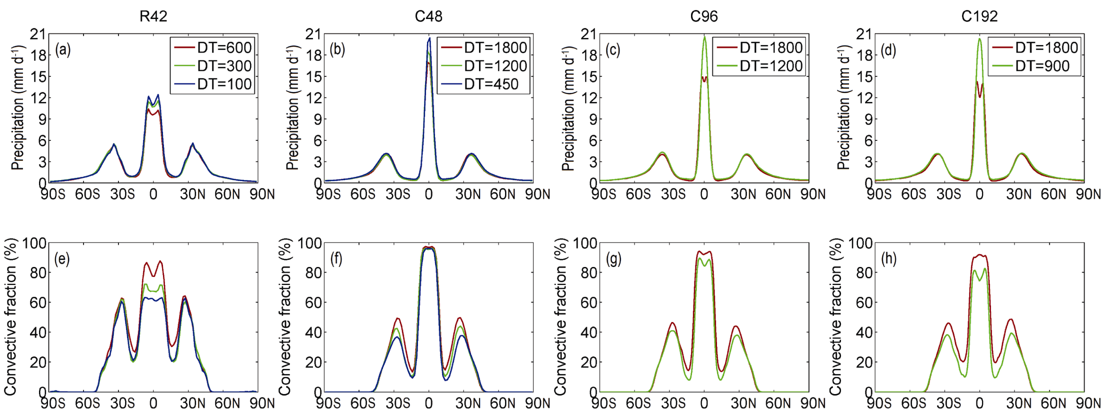

Figure 3 Upper panels: Time- and zonal-averaged precipitation determined by APEs with different time steps (DT) including (a) atmospheric models with a SAMIL and (b)–(d) those with a FAMIL. Bottom panels: Same as that in upper panels but for ratio of convective precipitation against total precipitation.

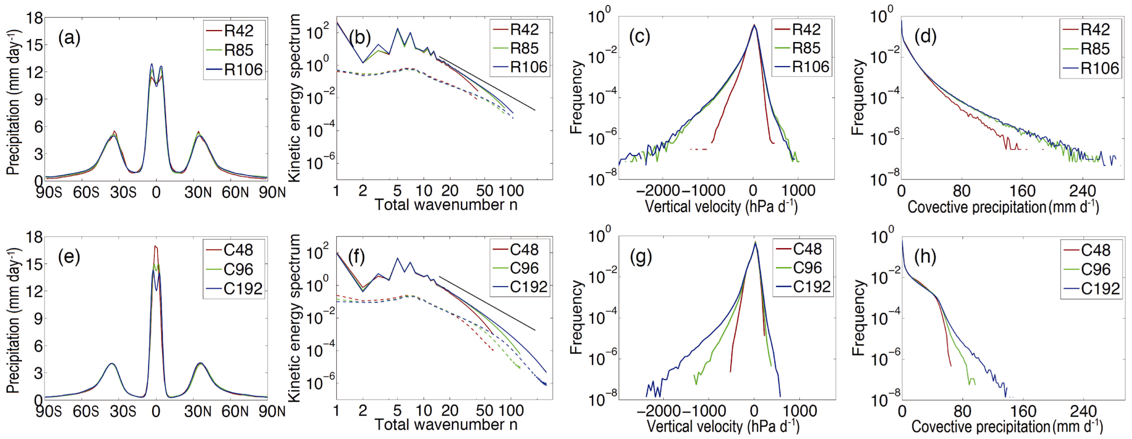

Figure 4 APEs including atmospheric models with a SAMIL, upper panels and those with a FAMIL, bottom panels at various resolutions. (a) and (e): Distributions of the zonal averaged precipitation. (b) and (f): Kinetic energy spectrum (approximately 200 hPa) on the two-dimensional wavenumber *n*. Dashed lines in (b) and (f) represent divergence components. Black lines in (b) and (f) are reference lines with a slope of –3. (c) and (g): Probability distributions of daily tropical vertical velocity (850 hPa, 30°S–30°N). (d) and (h): Probability distributions of daily tropical precipitation (30°S–30°N).

2011; Emori and Brown, 2005). As shown in Figs. 4c and 4g, the increase in horizontal resolution caused a broader probability distribution of daily vertical velocity, which indicates stronger extremes of upward and downward motions. Such vertical velocity extremes are generally associated with atmospheric motions at a scale near the grid interval. As the horizontal resolution increases, weaker diffusive smoothing is required for maintaining computational stability and a reasonable kinetic energy spectrum (Table 1) to resolve the small-scale kinetic energy, particularly the convergence component (Figs. 4b and 4f). Such processes are sub-grid and cannot be explicitly resolved in lower horizontal resolution simulations. Therefore, a higher horizontal resolution model could resolve additional convergence energy near the grid interval scale, and thus vertical velocity extremes, resulting in stronger convective precipitation generally corresponding to a scale close to the grid interval.

5 Conclusions and discussions

A series of control APEs were conducted for F/SAMIL to study the sensitivity of precipitation on dynamical core, time-step length, and horizontal resolution.

Sensitivity to the sensible heating of the equatorial maximum SST was stronger in FAMIL than that in SAMIL. The stronger surface sensible heating and larger low-level water vapor content in FAMIL led to larger CAPE and heavier equatorial rainfalls. The equatorial enhanced convections in FAMIL caused condensation heating to occur at a higher altitude. As a result, FAMIL usually formed strong maximum precipitation with a single peak over the equator, while SAMIL simulated weak double peaks in the tropics.

Moreover, the zonal averaged precipitation showed remarkable sensitivity to time step. When the time step was increased, the magnitude of the maximum precipitation over the equator decreased, particularly the large-scale precipitation fraction, and the single equatorial peak of FAMIL split into double peaks. Further studies showed that a longer time step created more time for the low-level atmosphere to produce and consume the CAPE, which led to stronger convection away from the equator, resulting in double peaks and a large convective fraction in the tropics.

Further, the probability distribution of precipitation, rather than the zonal mean, showed sensitivity to the horizontal resolution such that the precipitation extremes increased with increasing horizontal resolution. Higher resolution associated with weaker diffusive smoothing enabled more small-scale convergence energy to be resolved. Thus, more vertical motions associated with the extreme event were resolved, which led to more extreme vertical velocity and stronger precipitation extremes, particularly those of convective precipitation.

Previous studies showed that precipitation in APEs is also sensitive to the convection scheme. Lee et al. (2003) simulated the dependence of interseasonal oscillation on the cumulus parameterization. Moreover, Hess et al. (1993) showed the sensitivity of the intertropical convergence zone to Kuo parameterization and moist convective adjustment. Because the physical package used here was fixed, it is necessary to explore the sensibility on parameterization coupled with the dynamical core. The dependences of precipitation on the advection scheme and vertical resolution are also meaningful issues for further study.

Acknowledgements. This research is supported by the Chinese Academy of Sciences (XDA11010402 and XDA05110303), the National Basic Research Program of China (973 Program, 2012CB417203 and 2013CB955803), and the National Natural Science Foundation of China (91337110 and 41023002).

References

Arakawa, A., and W. H. Schubert, 1974: Interaction of a cumulus cloud ensemble with the large-scale environment. Part I, *J. Atmos. Sci.*, **31**, 674–701.

Bao, Q., P. Lin, T. Zhou, et al., 2013: The flexible global ocean-atmosphere-land system model, spectral version 2: FGOALS-s2, *Adv. Atmos. Sci.*, **30**, 561–576, doi:10.1007/s00376-012-2113-9.

Brinkop, S., and E. Roeckner, 1995: Sensitivity of a general circulation model to parameterizations of cloud-turbulence interactions in the atmospheric boundary layer, *Tellus A*, **47**, 197–220.

Emori, S., and S. J. Brown, 2005: Dynamic and thermodynamic changes in mean and extreme precipitation under changed climate, *Geophys. Res. Lett.,* **32**, L17706, doi:10.1029/2005GL023272.

Gregory, D., R. Kershaw, and P. M. Inness, 1997: Parameterization of momentum transports by convection. II: Tests in single-column and general circulation models, *Quart. J. Roy. Meteor. Soc.*, **123**, 1153–1183.

Hess, P. G., D. S. Battisti, and P. J. Rasch, 1993: Maintenance of the intertropical convergence zones and the large-scale tropical circulation on a water-covered earth, *J. Atmos. Sci.*, **50**, 691–713.

Houze, R. A. Jr., 2012: Orographic effects on precipitating clouds, *Rev. Geophys.*, **50**, RG1001, doi:10.1029/2011RG000365.

Lee, M. I., I. S. Kang, and B. E. Mapes, 2003: Impacts of cumulus convection parameterization on aqua-planet AGCM simulations of tropical intraseasonal variability, *J. Meteor. Soc. Japan*, **81**, 963–992.

Li, F., W. D. Collins, M. F. Wehner, et al., 2011: Impact of horizontal resolution on simulation of precipitation extremes in an aqua-planet version of Community Atmospheric Model (CAM3), *Tellus*, **63**A, 884–892.

Li, J. D., 2009: *Numerical Simulation Research of Radiation Process in Spectral Atmospheric Model of LASG/IAP (SAMIL)* (in Chinese), PhD's thesis, Institute of Atmospheric Physics, Chinese Academy of Sciences, 118pp.

Lin, S. J., 2004: A "vertical Lagrangian" finite-volume dynamical core for global models, *Mon. Wea. Rev.*, **132**, 2291–2307.

Neale, R. B., and B. J. Hoskins, 2000: A standard test for AGCMs including their physical parametrizations. I: The proposal, *Atmos. Sci. Lett.*, **1**, 101–107.

Nordeng, T. E., 1994: *Extended Versions of the Convection Parametrization Scheme at ECMWF and Their Impact Upon the Mean Climate and Transient Activity of the Model in the Tropics*, Research Dept Technical Memorandum No. 206, ECMWF, S. Park (Eds.), Reading, 41pp.

Pope, V. D., and R. A. Stratton, 2002: The processes governing horizontal resolution sensitivity in a climate model, *Climate Dyn.*, **19**, 211–236.

Putman, W. M., and S. J. Lin, 2007: Finite-volume transport on various cubed-sphere grids, *J. Comput. Phys.*, **227**, 55–78.

Song, X. L., 2005: *The Evaluation Analysis of Two Kinds of Mass-Flux Cumulus Parameterization in Climate Simulation* (in Chinese), PhD's thesis, Institute of Atmospheric Physics, Chinese Academy of Sciences, 158pp.

Sun, Z. A., and L. Rikus, 1999: Parametrization of effective sizes of cirrus-cloud particles and its verification against observations, *Quart. J. Roy. Meteor. Soc.*, **125**, 3037–3055.

Tiedtke, M., 1989: A comprehensive mass flux scheme for cumulus parameterization in large-scale models, *Mon. Wea. Rev.*, **117**, 1779–1800.

Wang, P. F., and Z. Z. Wang, 2006: A parallelization scheme for atmospheric general circulation model, *Chinese J. Atmos. Sci.* (in Chinese), **30**, 519–525.

Wang, X. C., Y. M. Liu, G. X. Wu, et al., 2013: The application of flux-form semi-Lagrangian transport scheme in a spectral atmosphere model, *Adv. Atmos. Sci.*, **30**, 89–100.

Wang, Z. Z., J. Y. Mao, and G. X. Wu, 2008: The wavenumber-frequency characteristics of the tropical waves in an aqua-planet GCM, *Adv. Atmos. Sci.*, **25**, 541–554.

Wang, Z. Z., G. X. Wu, T. W. Wu, et al., 2004: Simulation of Asian monsoon seasonal variations with climate model R42L9/LASG, *Adv. Atmos. Sci.*, **21**, 879–889.

Wei, K., and Q. Bao, 2012: Projections of the East Asian Winter Monsoon under the IPCC AR5 scenarios using a coupled model: IAP-FGOALS, *Adv. Atmos. Sci.*, **29**, 1200–1214.

Williamson, D. L., 2008: Convergence of aqua-planet simulations with increasing resolution in the Community Atmospheric Model, Version 3, *Tellus*, **60**A, 848–862.

Williamson, D. L., and J. G. Olson, 2003: Dependence of aqua-planet simulations on time step, *Quart. J. Roy. Meteor. Soc.*, **129**, 2049–2064.

Wu, G. X., H. Liu, Y. C. Zhao, et al., 1996: A nine-layer atmospheric general circulation model and its performance, *Adv. Atmos. Sci.,* **13**, 1–18.

Zhou, L. J., Y. M. Liu, Q. Bao, et al., 2012: Computational performance of the high-resolution atmospheric model FAMIL, *Atmos. Oceanic Sci. Lett.*, **5**, 355–359.